RSC Advances

PAPER

View Article Online
View Journal | View Issue

Cite this: *RSC Adv.*, 2018, **8**, 13423

Impact of carboxylation and hydrolysis functionalisations on the anti-oil staining behaviour of textiles grafted with poly(*N*-isopropylacrylamide) hydrogel

Siti Samahani Suradi, Nurul Hazlina Naemuddin, Shahrir Hashim and Nadia Adrus *

Novel hydrogel-modified textiles have been prepared through photografting poly(*N*-isopropylacrylamide) (PNIPAAm) onto pristine and functionalised polyethylene terephthalate (PET) surfaces. In this work, two types of functionalisation, carboxylation (CPET) and hydrolysis (HPET), were performed to scrutinise the hydrogel grafting efficiency. Basic characterisation of the pristine, functionalised and grafted textiles was carried out *via* fourier transform infrared spectroscopy (FTIR), atomic force microscopy (AFM) and field emission scanning electron microscopy (FESEM) analyses. Then, the functional characteristics of these samples were determined based on the oil staining performance. Functionalisation of the PET textiles *via* hydrolysis and carboxylation gives rise to different chemical reactivity and interactions on the PET surface. Impressively, the surface formed *via* hydrolysis functionalisation of PET was found to be more efficient compared to that formed *via* carboxylation, and the untreated one. The HPET surface was remarkably more hydrophilised and rougher than both the UPET and CPET surfaces. The accessibility of the –OH groups for hydrogen abstraction from HPET has a great impact on the hydrogel grafting onto the HPET surface. All the grafted textiles (PNIPAAm-*g*-UPET, PNIPAAm-*g*-CPET and PNIPAAm-*g*-HPET) demonstrated anti-oil staining behaviour at 27 °C. In particular, PNIPAAm-*g*-HPET textiles with a high degree of grafting (DG) exhibited the fastest rate for oil to de-stain from the surface. Moreover, the reversible transition of PNIPAAm hydrogels around the lower critical solution temperature (LCST) ~ 32 °C from hydrophilic to hydrophobic generates switchable surfaces of the textiles with regard to the oil wettability. Specifically, PNIPAAm-*g*-HPET textiles also displayed the highest degree of wettability switching as a result of having the highest DG. Taken together, the PNIPAAm hydrogels grafted onto PET textiles were significantly enhanced though hydrolysis functionalisation and possessed excellent switchable surfaces toward oil-staining, having great potential to be used for applications in oil and water separation as well as smart textiles.

Received 31st January 2018
Accepted 25th March 2018

DOI: 10.1039/c8ra00959g

rsc.li/rsc-advances

1. Introduction

In recent years, the demand for the development of materials that can efficiently separate oil and water has aroused significant interest. Scientists have shifted their attention towards the development of 'water-removing' materials, which exhibit the opposite wettability to oil. This is because materials with special wettability possess multi-functionality, such as self-cleaning and anti-oil staining functions, which may find use in various applications including separation materials and smart textiles. Most recent approaches have been focused on the hydrophilic and oleophobic modification of several substrates with various coatings, including fluorinated polymers,[1,2] hydrophilic polymers,[3–5] inorganic materials[6–8] and nanoparticles.[9,10] As these hydrophilic–oleophobic materials show water wetting preferences over oils, they have significant advantages compared to traditional 'oil-removing' materials, such as good oil resistance and recyclability without requiring post-treatment.[11–13] Additionally, these materials are also easy to fabricate and have no limitation in terms of absorption capacity because the separation is based on a filtration mechanism. Since these hydrophilic/oleophobic filters have anti-oil wetting properties, this could lead to faster and higher efficiency filtration that is easily scalable for commercial applications.

Following this strategy, porous substrates, including meshes, polymer films, membranes and textiles, are good candidates for hydrophilic modification due to their large pore volume, flexibility and commercial availability.[7,14–16] These materials can be modified *via* coating[5,17] or grafting[18,19] methods. Xue *et al.* reported the use of metallic substrates for

Department of Bioprocess and Polymer Engineering, Faculty of Chemical and Energy Engineering, Universiti Teknologi Malaysia, 81310 UTM Johor Bahru, Johor, Malaysia. E-mail: nadia@utm.my

hydrogel coatings that can selectively and effectively (99%) separate water from an oil/water mixture.[4] Liu and co-workers previously coated polyvinylidene fluoride (PVDF) membranes with chitosan–silica nanoparticles using glutaraldehyde for effective oil/water emulsion separation.[20] Moreover, composite membranes based on PVDF/nano-sized titanium oxide cast onto a non-woven fabric as a substrate exhibit higher permeability and good fouling resistance.[21]

Despite much progress in this field and the existing hydrophilic/oleophobic modifications, detailed studies on the interplay between hydrogels and the chosen substrates *via* chemical functionalisation are still lacking. For example, current research is more focussed on the use of fluorinated compounds instead of hydrogels in order to enhance the special wettability of membrane coatings.[20,22] Most fluorinated compounds are harmful and quite costly.[23,24] Stainless steel meshes modified *via* physical coating using zinc oxide[25] or hydrogels[4,26] suffered from poor interfacial surface properties that could result in the coating delaminating from the substrate surface. This has become a drawback of the physical coating approach compared to the grafting process that limits its practical applications. Additionally, stainless steel meshes are difficult to graft due to the lack of reactive functional groups on their surface. In this regard, the grafting method is more suitable for modifying the surface chemistry of polymeric membranes and textiles. Polyethylene terephthalate (PET) textiles are one of the most commonly used substrates and possess excellent characteristics, including easily scalable modification, anti-wrinkle properties and flexibility.[27,28] However, it is always a challenge to modify the surface of PET textiles because of their hydrophobic surfaces. Hence, several techniques have been applied, including surface functionalisation *via* carboxylation and hydrolysis.[29–31] These techniques have been proven to impart more hydrophilicity and specific functionalities on PET surfaces, which can offer improvements in the chemical stability. Through these functionalisations, the incorporated functional moieties on these surfaces are tremendously effective for further grafting in order to achieve hydrophilic/oleophobic surfaces.

In this paper, we report the grafting of poly(*N*-isopropylacrylamide) (PNIPAAm) hydrogels onto functionalised PET textiles. Amongst hydrophilic materials, hydrogels are typically three-dimensional hydrophilic polymeric networks filled with large amounts of water. Due to their excellent water absorbing and water retaining capacities, hydrogels are highly efficient 'water-removing' materials. A smart temperature-responsive PNIPAAm hydrogel was chosen due to its fascinating 'sensor' properties, which can be reversibly switched from a hydrophilic to hydrophobic state across its lower critical solution temperature, LCST $\sim$ 32 °C. To use this smart hydrogel effectively, we grafted it onto a PET substrate in order to generate a more stable hydrophilic and oleophobic modification *via* a fluoride-free approach.[32] Importantly, efforts were made to make the PET surface more compatible with the PNIPAAm hydrogel using a systematic functionalisation strategy *via* carboxylation and hydrolysis.[33,34] The surface functional groups, roughness and morphology were investigated in detail. These surface functionalisations on the PET substrates provide different surface properties and interactions with the grafted hydrogel. We have demonstrated that carboxylation and hydrolysis give rise to different accessibility of the hydroxyl groups on the PET surface, further enhancing grafting with the PNIPAAm hydrogel, which can ultimately improve the resistance towards oil staining, making the material easily recyclable and recoverable with excellent switchable wetting $\leftrightarrow$ anti-wetting surfaces.[35–37] Overall, this study suggests a facile and new technique to design modified PET textiles that could potentially be used for oil and water separation applications as well as smart textiles.

2. Experimental section

2.1. Materials

N-Isopropylacrylamide (NIPAAm) monomer, *N*,*N*′-methylenebisacrylamide (MBAAm) crosslinker, benzophenone (BP; "type II" photoinitiator), sodium hydroxide (NaOH), potassium permanganate ($KMnO_4$), hydrochloric acid (HCl, 37%), sulphuric acid (H_2SO_4, 96%) and acetic acid (CH_3COOH, 99%) were purchased from Acros Organic (Belgium), Sigma-Aldrich (USA), Rahn AG (Germany) and Fisher Scientific (M) Sdn. Bhd. (Malaysia). All chemicals were analytical grade with high purity. NIPAAm was recrystallised from *n*-hexane while other chemicals were used directly without further purification. The PET nonwoven textile was supplied by Feichang Lianyi Engineering, China.

2.2. Surface functionalisation of PET textiles

The PET textiles were cut into circles with a diameter of 4.5 cm and washed with distilled water to remove the impurities. The hydrolysis functionalisation was carried out by immersing the untreated PET (UPET) textiles into NaOH solution (1 N) at 60 °C for 2 hours. Then, the PET textiles were rinsed with abundant water to remove any traces of alkali on the surface of the textiles. After the treatment, the textiles were neutralised with a dilute CH_3COOH solution and were washed again with distilled water. Finally, the treated textiles were dried at room temperature for 48 hours. Alternatively, the carboxylation functionalisation was carried out through the immersion of UPET textiles in a reaction mixture of 10 g $KMnO_4$ in 200 mL H_2SO_4 (0.75 N), for about two and a half hours. Then, the textiles were washed twice with deionised water. Next, the PET textiles were submerged in HCl (6 N) four times. The PET textiles were washed again with water four times and twice with ethanol before being dried in oven at a temperature of 45.8 °C overnight.

2.3. Surface grafting of PNIPAAm onto PET textiles

The photoinitiator type II solution was prepared using 50 mM BP in 10 mL of C_2H_5OH. All the samples of UPET and functionalised PET (carboxylation: CPET, and hydrolysis: HPET) textiles were immersed in the photoinitiator solution for 1 hour. Meanwhile, the PNIPAAm pre-gel reaction mixture was prepared using purified AAm (15 wt%) in 5 mL of distilled water, followed by the addition of MBAAm (crosslinker, 5 wt%), and

this was stirred until completely dissolved. The textiles were immersed for about 15 minutes in the pre-gel solution and exposed to UV LED light (UV LED, Hönle UV Technology, Germany) for 20 minutes.

2.4. Degree of grafting

After the irradiation step, the textile samples were equilibrated with distilled water for 8 hours to elute all the unreacted monomer, BP and homopolymer. Then, the textile samples were dried in oven at 45 °C for about 24 hours and weighed again. The degree of grafting (DG) for PNIPAAm-*g*-UPET, PNIPAAm-*g*-CPET and PNIPAAm-*g*-HPET was determined using eqn (1):

$$\mathrm{DG} = \frac{W_\mathrm{f} - W_\mathrm{i}}{W_\mathrm{i}} \times 100\% \quad (1)$$

where W_i is the initial weight of the textile sample and W_f is the textile weight after functionalisation.

2.5. PET surface characterisation

The functional groups on the surface of UPET, functionalised PET (CPET and HPET), and grafted PET (PNIPAAm-*g*-UPET, PNIPAAm-*g*-CPET, PNIPAAm-*g*-HPET) were analysed using a fourier transform infrared spectrophotometer (FTIR, Perkin Elmer Spectrum One) *via* a potassium bromide (KBr) pellets standard technique. The spectra were obtained in the region 4000–600 cm^{-1} in transmittance mode for 32 scans. Samples were prepared by dispersing the complexes well in KBr and compressing the mixtures to form disks. The surface topographies of the PET textiles were evaluated using an atomic force microscopy (AFM, Nanoscope IIIA) system in tapping mode with a silicon nitride probe. The morphological structures of the surfaces of the as-prepared samples were investigated using field emission scanning electron microscopy (FESEM, JEOL JSM-6701F) at a voltage of 5 kV. These samples were coated with gold and the surface features were visualised individually at different magnifications. Water contact angle (WCA) measurements of the PET textiles were performed using an optical contact angle measurement system (VCA Optima) using the sessile drop technique at 27 and 45 °C. A water droplet (2.0 μL) was dropped onto the surface of the as-prepared samples and readings were recorded three times for each sample.

2.6. Anti-oil staining assessment

For this investigation, cooking oil was selected as a model pollutant in the water source and the assessment was carried out at 27 and 45 °C. Pictures of the grafted PET textiles after dipping in oils and washing with water were captured. The recyclability of the grafted PET samples was determined based on the time taken for the oil to disappear at 27 °C after 5 cycles.

3. Results and discussion

3.1. Preparation of functionalised PET textiles

The PET textiles were chemically functionalised to improve the surface hydrophilicity and surface roughness, and to enhance the efficiency of the subsequent surface-initiated grafting photopolymerisation because accessible reactive functional groups were introduced. The reactive functional groups were generated depending on the chemical functionalisation approach. The carboxylation and hydrolysis functionalisations favoured enhancing the carboxyl and hydroxyl groups, respectively.[29] Basically, the structure of pure PET consists of a substantial amount of hydroxyl and carboxyl groups. The carboxylation or hydrolysis process creates a higher amount of hydrophilic chain-ends *via* selective cleavage of the PET ester bonds.[38] The hydrolysis process introduced more hydroxyl groups in the chain-ends of the HPET surface when the PET ester bonds were cleaved (*cf.* Scheme 1(A)).[31,38] These reactive functional surface groups are useful for immobilizing the BP initiator on the functionalised PET surface and become active sites for the subsequent surface grafting of PNIPAAm-*g*-PET textiles.[29] Meanwhile, more carbonyl-carboxyl groups were formed in the CPET end chains. Thus the ester groups at the CPET surface converted to mostly carboxyl groups (*cf.* Scheme 1(B)).[29,38]

FTIR analysis was employed to characterise the functional groups on the PET textile surfaces. The FTIR spectra of unmodified PET (UPET) and functionalised PET textiles made *via* carboxylation and hydrolysis (CPET and HPET) are shown in Fig. 1. Even though all of the PET textiles displayed characteristic bands with similar peak positions in each spectrum, the spectra of the textiles after functionalisation certainly exhibited different peak intensities. Peaks were detected at 1746–1635, 1410 and 1343 cm^{-1}, which correspond to the stretching of the carbonyl bonds (–C=O), and the bending and wagging modes of the ethylene units, respectively. The appearance of broad absorption bands at around 3420 cm^{-1} was attributed to the intermolecular –OH bonded to the C=O groups and –OH of the carboxylic groups in the PET chains.[39] Three strong stretching vibrations were identified at 1235, 1090 and 1017 cm^{-1}, and are mainly attributed to the PET ester bonds.[40]

When compared to that of the UPET textile, the spectrum for CPET (Fig. 1) shows weaker intensity absorption bands at

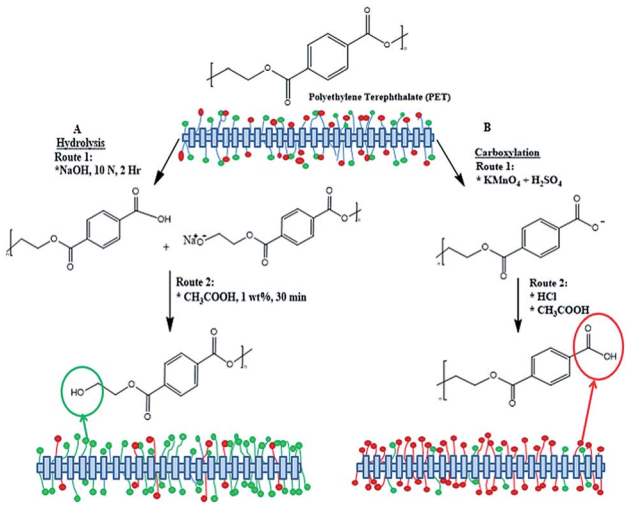

Scheme 1 Surface functionalisation *via* carboxylation (right) and hydrolysis (left) of polyethylene terephthalate.

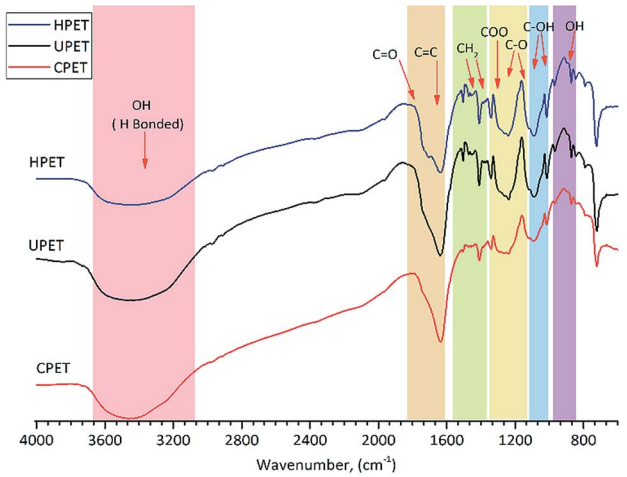

Fig. 1 The FTIR spectra of UPET, CPET and HPET in the absorption range 4000–600 cm^{-1}.

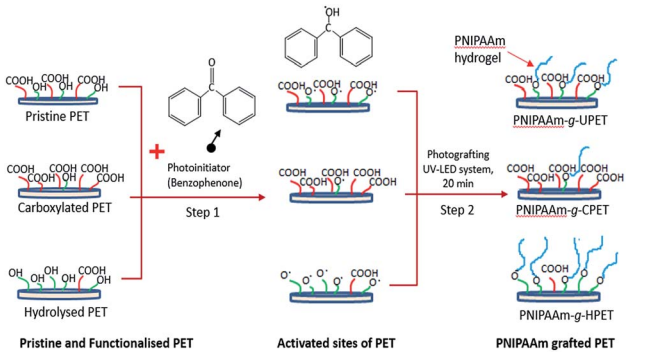

Scheme 2 Schematic diagram of the steps of grafting the PNIPAAm hydrogel onto the PET textile surface.

around 1746 and from 1123 to 1090 cm^{-1}. The alteration of CPET was indicated by the fading ester groups at around 1235 cm^{-1}. It can also be observed that the ester peaks of PET diminished at around 1710 and 910 cm^{-1} after carboxylation. This indicates that the ester bonds of PET were cleaved during carboxylation.[29,38] Only the carboxyl groups remained at the end of the polymer chains.

Meanwhile, carboxyl (COO^-) and hydroxyl (–OH) groups were found on the HPET textile similar to on the CPET (Fig. 1) due to the cleavage of the PET ester bonds. Hydrolysis functionalisation forms more hydroxyl groups rather than carboxyl groups. The appearance of a shoulder at around 1710 cm^{-1} indicates the formation of hydrogen bonds to the surface of the hydrolysed PET (HPET). At the same time, the peaks at 1505, 1174, 1090, 1017, and 910 cm^{-1} (Fig. 1, HPET) were intensified, and are assigned to C=C, C–O and –OH groups, respectively. Apparently, the spectrum of HPET exhibits broader and higher adsorption peaks than that of UPET at the following peak positions: 1746, 1174, and 910 cm^{-1}. The decrease in the intensity of the HPET adsorption bands at 1235, 1090 and 1017 cm^{-1} could also be an indication that the ester bonds of PET were cleaved *via* hydrolysis. The FTIR data revealed that the HPET consists of a higher amount of hydroxyl groups and becomes more hydrophilic, which could further enhance the grafting of the PNIPAAm hydrogel onto PET.[41]

3.2. Preparation of PNIPAAm-*g*-PET textiles

The surface grafting of the PNIPAAm hydrogel onto PET is a subsequent step after the functionalisation of the PET textiles. Here, the 'grafting-from' approach was applied to grow more polymer chains on the PET surfaces. This approach consists of two steps: (i) pre-adsorption of the photoinitiator onto the PET surface, and (ii) subsequent graft polymerisation of the PNIPAAm hydrogel onto the PET surface *via* photoinitiated hydrogen abstraction, as depicted in Scheme 2. For this purpose, the unmodified and functionalised PET textiles were employed as substrates to be grafted with the PNIPAAm hydrogel.

First, the BP molecules were immobilised and adsorbed onto the PET surface. Then, UV LED light was used as a light source to excite the BP photoinitiator at 365 nm. This led to hydrogen abstraction of the functional group to form free radicals on the surface.[42,43] After reactive sites were produced, these high energy radicals initiated the graft photopolymerisation in the subsequent step.[29,44] Thus, the growth of the PNIPAAm chains was propagated in relation to the accessible amount of reactive groups that were introduced during primary functionalisation.[43]

Immobilisation of the photoinitiator on the PET textiles with different functionalities had an influence on its pre-adsorption onto the surface. UPET has a comparatively equal amount of carboxyl and hydroxyl functional groups. After functionalisation, HPET consisted of a hydroxyl-rich terminated surface, while CPET had a higher amount of carboxyl end groups compared to the uncleaved PET base material. The pre-adsorption of the BP initiator on the HPET surface was significantly improved by the interactions of the hydroxyl groups of the surface and the photoinitiator. The increase in the number of accessible hydroxyl groups on HPET, which were introduced during hydrolysis, enabled efficient hydrogen abstraction with the aid of the BP photoinitiator. This could lead to more efficient and selective functionalisation, resulting better control of the DG of the PNIPAAm hydrogel onto the HPET surface. Alternatively, the UPET could be modified much more efficiently than CPET. This can be explained by the fact that the surface of the CPET textile was shielded by the carboxyl groups and therefore the formation of free radicals *via* hydrogen abstraction was hindered. A similar finding was reported by Geismann and colleagues.[29] This study has shown that the formation of active sites on the PET surface was influenced by the hydrogen abstraction from the selective reactive functional groups *via* a photoinitiator pre-adsorption approach. Hence, the functionalised PNIPAAm-*g*-PET textiles made *via* grafting could be tailored accordingly. To confirm this further, the effect of functionalisation *via* carboxylation and hydrolysis of the PET textiles on the photografting polymerisation of PNIPAAm can be scrutinised based on the DG results (*cf.* Section 3.3).

The surface of the unmodified and functionalised PET textiles after grafting photopolymerisation was characterised by means of FTIR analysis. By referring to the adsorption peaks of ungrafted PET (Fig. 1), a dramatic change of the spectra can be clearly seen for the grafted PET textiles, as shown in Fig. 2. New peaks associated with the characteristic peaks of the PNIPAAm hydrogels appeared on the spectra of the grafted PET, which are detected at wavenumbers of 1635, 1535, 1170 and 1090 cm^{-1}. These peaks were attributed to the C=O (amide I), C–N (amide II) and OH groups, respectively. A broader and stronger band around 3454 cm^{-1} was also detectable, which corresponds to the stretching vibrations of the –OH group overlapped with the N–H stretching vibration bands for the PNIPAAm hydrogel.[45] Additionally, medium peaks at 1453 and 1338 cm^{-1}, which are assigned to the stretching vibrations of the isopropyl groups of PNIPAAm, were also seen.[46,47] Therefore, the presence of PNIPAAm absorption bands has confirmed that the grafting of the PNIPAAm hydrogel layer onto the surface of the PET textiles was successful.

The effect of grafting on the PET textiles after carboxylation and hydrolysis functionalisation (PNIPAAm-*g*-CPET and PNIPAAm-*g*-HPET) was also studied using FTIR analysis, and the results are shown in Fig. 2. The characteristic absorbance bands at around 3454, 1635 and 1535 cm^{-1} in these IR spectra validate that the PNIPAAm hydrogel layer was grafted onto the CPET and HPET during photopolymerisation. When compared to those of PNIPAAm-*g*-UPET, the transformation of the peaks of PNIPAAm-*g*-CPET and PNIPAAm-*g*-HPET can clearly be identified. PNIPAAm-*g*-HPET shows broader amide (I) and amide (II) peaks with absorption bands around 3454, 1713 and 1241 cm^{-1} (Fig. 2). The intensity of the PNIPAAm-*g*-HPET peaks at 1235, 1090 and 910 cm^{-1} (ester group) is diminished, which clearly emphasised that the surface of HPET was significantly covered with a grafted layer of the PNIPAAm hydrogel. Furthermore, an increase in the intensity of the PNIPAAm-*g*-HPET peaks at 1645 and 1575 cm^{-1} suggested that more hydrogen bonding had occurred. This noticeably shows that the grafting of the PNIPAAm hydrogel onto the HPET surface is relatively enhanced compared to that on the UPET surface (Fig. 2). However, the presence of characteristic PET bands (*cf.* Fig. 1) around 1746, 1235, 1174, 1090 and 1017 cm^{-1} can still be seen in the PNIPAAm-*g*-CPET. The remaining PET functional groups on the surface reveal that only a small amount of the PNIPAAm hydrogel layer was grafted onto PNIPAAm-*g*-CPET, when compared to on both PNIPAAm-*g*-HPET and PNIPAAm-*g*-UPET. This is in agreement with the effect of carboxylation explained earlier; the CPET textile was shielded by the carboxyl groups during grafting photopolymerisation.

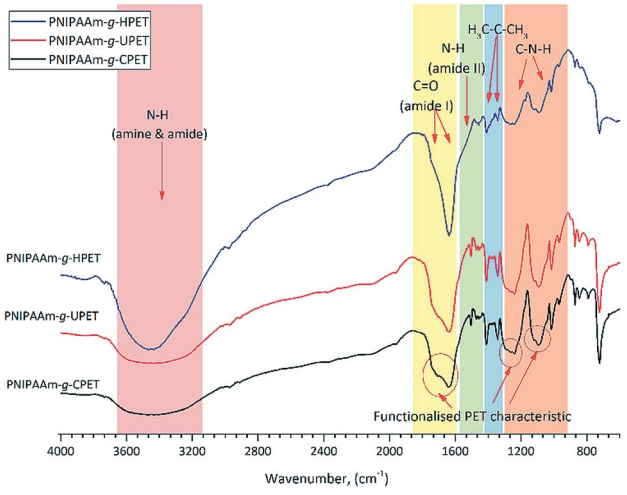

Fig. 2 The FTIR absorptions of the various PNIPAAm hydrogel grafted functionalised PET textiles, PNIPAAm-*g*-UPET, PNIPAAm-*g*-CPET and PNIPAAm-*g*-HPET, in the absorption range 4000–600 cm^{-1}.

3.3. Characterisation of PET textiles

To further confirm that the PNIPAAm hydrogel was grafted onto the PET surfaces, we also conducted a quantitative analysis based on the percentage DG, and the results are shown in Fig. 3. After the grafting functionalisation has taken place, the PET textiles were covered with a PNIPAAm layer that contributed to the DG value. We found that the amount of PNIPAAm hydrogel grafted onto the pristine UPET surface was 15.5% on average. Meanwhile, the amounts of PNIPAAm hydrogel grafted onto the functionalised CPET and HPET were 5.1% and 33.2%, respectively (Fig. 3). The trend obviously shows that the amount of PNIPAAm grafted onto HPET (PNIPAAm-*g*-HPET) was the greatest. We have noted that the hydrolysed surface has highest tendency for grafting, rather than the UPET and CPET textiles. This suggests that the development of more hydroxyl groups at the end chains of HPET made it more susceptible to hydrogen abstraction by the BP initiator upon UV irradiation. In addition, the surface of HPET tended to be highly hydrophilic. This could also provide better compatibility with hydrogel materials[30,48] and thus, the grafting of the PNIPAAm hydrogel onto the PET surfaces was further enhanced. In contrast, the PNIPAAm hydrogel grafted onto the CPET surface displayed the lowest DG value, which was even significantly lower than that of PNIPAAm-*g*-UPET. This shows a clear correlation between the DG and the amount of accessible carboxyl groups on the CPET surface. The

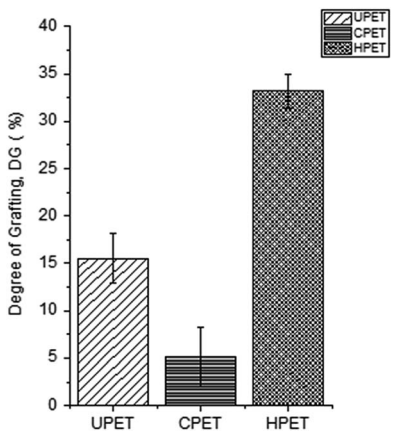

Fig. 3 The degree of grafting of the PNIPAAm hydrogel grafted onto PET with different functionalisations.

shielding effect of the CPET surface reduced the efficiency of hydrogen abstraction by the BP initiator for efficient grafting due to the limited accessibility of the carboxyl groups after the carboxylation.[29]

The surface roughness plays a key role in elucidating the effect of chemical functionalisation and grafting onto PET surfaces. For this purpose, AFM analysis of the PET textiles was conducted in the dry state. The distinctive topographies of the pristine UPET and functionalised PET textiles are shown in Fig. 4, with the light regions being the highest points and the dark regions representing the depth of the valleys. The surface roughness data for the PET after functionalisation and grafting processes were obtained based on the root mean square average roughness (R_{ms}), as stated in Fig. 4. When comparing with the pristine UPET as a benchmark, a substantial change of the roughness of the PET surfaces was observed (area of 2 μm × 2 μm, *cf.* Fig. 4). After functionalisation, the R_{ms} of the PET surfaces was gradually increased from 3.341 nm to 10.50 nm. The pristine UPET shows a smooth surface of irregular curvatures, which is illustrated by the bright peaks and dark valleys (Fig. 4a).[49,50] The surface curvature and distribution of protrusions for both the functionalised PET surfaces are relatively different.[51] The CPET surface possesses a regular curvature and uniform distribution of peak to valley topography with isolated growth of micro- and nano-grooves (Fig. 4b). Meanwhile, the surface roughness of HPET has consistently increased. This indicates that etching of the HPET textile surface *via* hydrolysis has occurred, resulting in a topography with numerous protrusions and grooves (Fig. 4c). The results from our study are corroborated by previous work by Škvarla and co-workers; the PET surface became increasingly eroded *via* hydrolysis.[51] An increase in the surface roughness is important for improving the interfacial adhesion of the PNIPAAm hydrogel onto the HPET surface in the subsequent functionalisation.[52,53]

The topography of the PET textiles after the grafting process is shown in Fig. 4d–f. Even though the PNIPAAm-*g*-UPET surface shows heterogeneous curvature similar to that of UPET, the uneven distribution of lumps and significantly larger R_{ms} value could also be noted. This is an indication that the PNIPAAm hydrogel was grafted onto the UPET surface.[54] The PNIPAAm-*g*-CPET exhibited the lowest R_{ms} value; its surface is less rough with a uniform distribution of small pits. The surface also displayed a less pronounced peak to valley topography (Fig. 4e).[55] This can be elucidated by the fact that the hydrogen abstraction by the carboxyl groups in the primary functionalisation (CPET) occurred in shielded manner, thus only a low concentration of energy-rich starter radicals were formed.

Consequently, this resulted in a lesser extent of grafting polymerisation causing the smoother surface of PNIPAAm-*g*-CPET.[56] In contrast, the topography of PNIPAAm-*g*-HPET (Fig. 4f) displayed prominent roughening with numerous protrusions and grooves, which is consistent with the R_{ms} value. The PNIPAAm-*g*-HPET surface was constructed of micro-scale bulges with deeper curvatures. The functionalisation *via* hydrolysis improved the PET roughness and enhanced the amount of accessible hydroxyl groups on the HPET surface, stimulating more PNIPAAm hydrogel to be grafted onto the HPET surface.[54,57] This finding is also in agreement with the DG results.

The effects of functionalisation and the subsequent grafting process on the PET surfaces were further investigated using FESEM analysis at three different magnifications, as shown in Fig. 5 and 6. The FESEM images at 500× magnification show the random stacking orientation of the PET fibres constructing

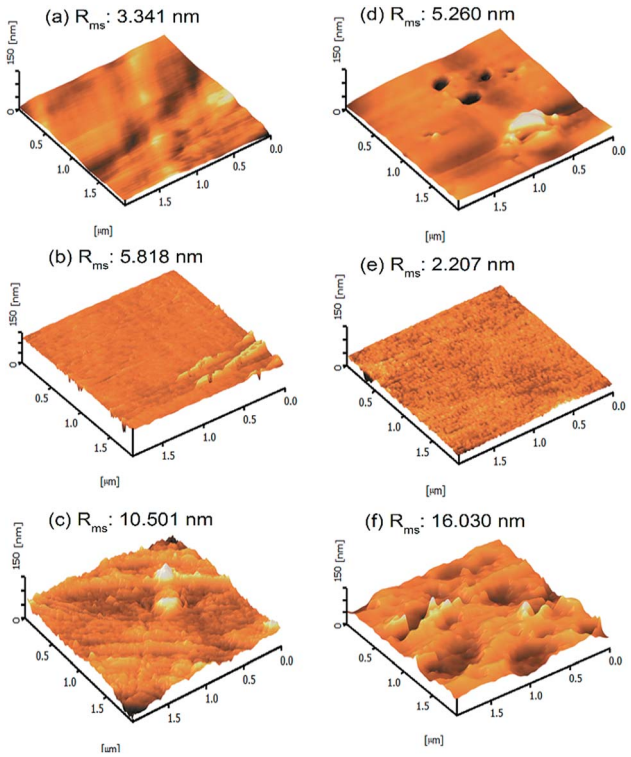

Fig. 4 The AFM images of PET textiles before grafting; (a) UPET, (b) CPET and (c) HPET, and the PET textiles after grafting with the hydrogel; (d) PNIPAAm-*g*-UPET, (e) PNIPAAm-*g*-CPET and (f) PNIPAAm-*g*-HPET. The measurements were carried out at 25 °C.

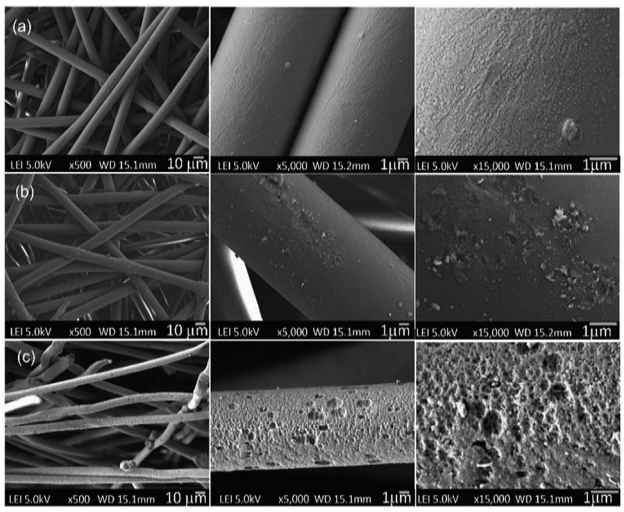

Fig. 5 Surface morphologies of the PET textiles before and after functionalisation; (a) UPET, (b) CPET and (c) HPET, based on a top view.

mesh-like voids. The morphology of a single fibre and its top surface are shown by further zooming at 5 000× and 15 000× magnification, respectively.

As a benchmark, the UPET textile appears to have a smooth sandy surface with orderly aligned wrinkles along the fibre axis structure (Fig. 5a). This is in agreement with previous studies.[31,58] After primary functionalisation steps, the surface morphologies of the PET textiles were not significantly altered *via* carboxylation, but were drastically changed *via* hydrolysis.[59] Overall, the surface of CPET appeared much smoother than that of the pristine PET, with isolated aggregations of small pits. In contrast, the HPET is significantly more porous than the pristine UPET. Hydrolysis creates remarkable roughness and cavities on the HPET surface.[31,51] This can be attributed to the etching of pristine PET textiles during the functionalisation reaction, resulting in the exposed structure of the PET surfaces. Similar findings have also been reported by researchers previously.[31,58]

As shown in Fig. 6a–c, obvious changes of the morphologies of the PET surfaces can be observed after the grafting photopolymerisation process has taken place. This observation indicates that the PNIPAAm hydrogel layer was successfully grafted onto the PET surface. As a remark, the FESEM images were obtained under dry conditions. At a lower magnification, we observed a transparent film covering the voids between the PET fibres, which may represent the hydrogel layer. From the high-magnification FESEM images, the entire PNIPAAm-*g*-UPET (Fig. 6a) surface exhibited a moon-surface morphology with a moderately rough appearance. In contrast, only a few regions of PNIPAAm-*g*-CPET were covered with a bumpy appearance. The hindrance of the carboxyl groups to forming starter radicals *via* hydrogen abstraction has resulted in less grafting and heterogeneous distribution of the hydrogel layer.

Meanwhile, the increase in the surface porosity and cavities of HPET provided a free area for the PNIPAAm hydrogel to be easily grafted onto it. The attachment of the PNIPAAm hydrogel onto the HPET surface covered both the cavities and pores on the surface as well as the mesh-opening of the voids, thus the HPET surface appeared smoother after grafting (Fig. 6c).[55,60] Up to this point, the change in surface morphology clearly supports the reasoning behind the DG results and surface roughness determined *via* AFM analysis, for all the PET textiles before and after grafting.

3.4. Oil staining behaviour at different temperatures

The oil staining resistance of the PNIPAAm hydrogel grafted PET textiles was examined in order to assess the performance with regard to oil fouling. For this purpose, three different grafting samples, PNIPAAm-*g*-UPET, PNIPAAm-*g*-CPET and PNIPAAm-*g*-HPET, were immersed in oil for about two minutes and subsequently washed with water. The measurements were carried out at temperatures below and above the LCST of PNIPAAm, *i.e.* 27 and 45 °C, respectively. The oil staining resistance was assessed qualitatively and quantitatively from (i) the appearance of the textiles without and with hydrogel grafting, and (ii) the times taken for the oil to disappear from the grafted PET textiles when immersed in water at a temperature of 27 °C. Images of the UPET textiles before and after oil staining are shown in Fig. 7. During the testing, the oil spread instantaneously upon contact with the UPET textile. Not only that, the UPET textile was completely stained with oil and the staining was unremovable (Fig. 7b). Regardless of the temperature, the UPET textile was susceptible to oil staining due to its permanent oleophilic and hydrophobic surface.

In addition, the appearances of the grafted PET textiles (PNIPAAm-*g*-UPET, PNIPAAm-*g*-CPET and PNIPAAm-*g*-HPET) after oil staining were also assessed, as shown in Fig. 8. Note that this testing was conducted for 5 cycles at 27 and 45 °C. The PNIPAAm hydrogel grafted PET textiles were in swollen states when immersed in oil below the LCST (27 °C). The physical appearances of these three different grafted PET surfaces after 5 cycles of testing are consistently clean without significant oil staining (Fig. 8ii). In the swollen state, the grafted PET textiles generate a hydration layer, thus preventing oil adhesion on the PET surfaces. The sufficient hydration layer in the swollen state caused steric repulsion to effectively repel oil adsorption on the surface.[61,62] The correlation between the strong hydration of the

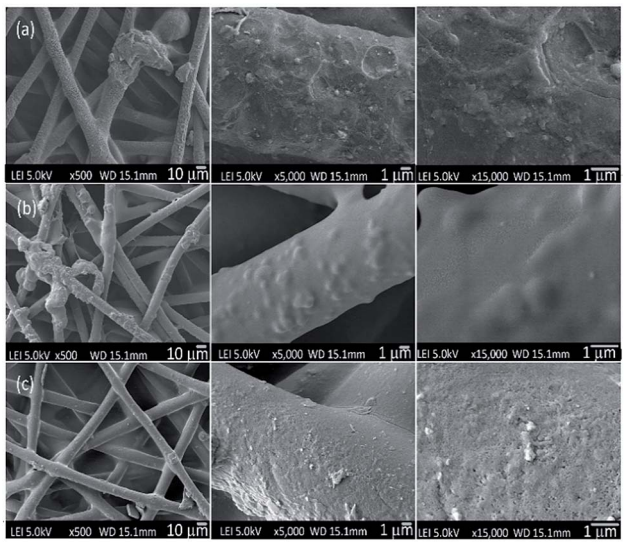

Fig. 6 Surface morphologies of the PET textiles after grafting; (a) PNIPAAm-*g*-UPET, (b) PNIPAAm-*g*-CPET, and (c) PNIPAAm-*g*-HPET, based on a top view.

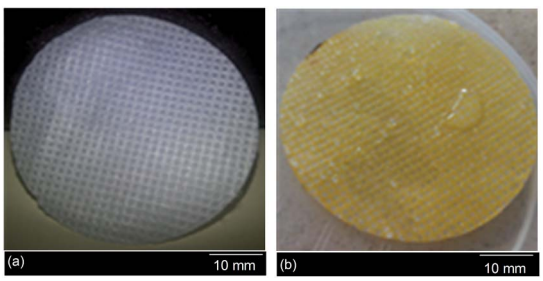

Fig. 7 The appearance of the unmodified PET textile; (a) the clean surface before oil staining, and (b) the permanent and irreversible oil stained surface even after intensive washing with water.

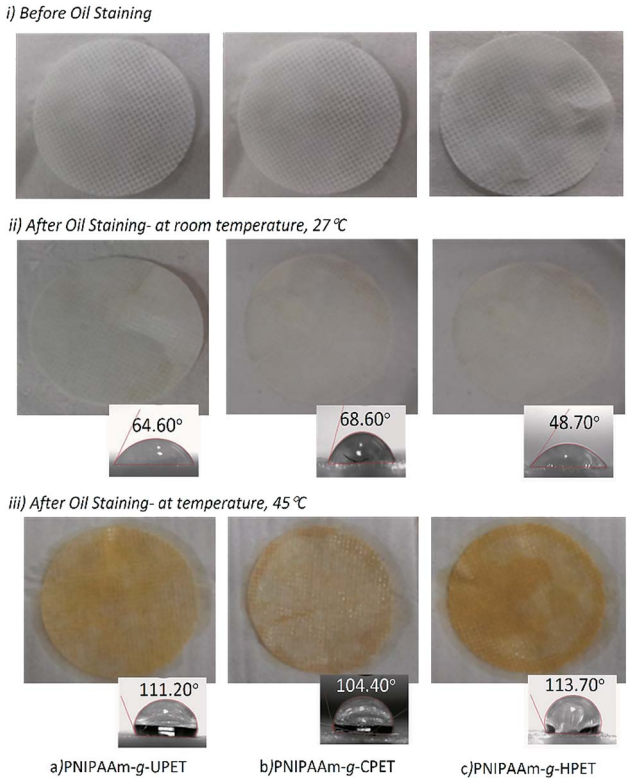

Fig. 8 The effect of oil staining before and after immersion in oil at 27 and 45 °C on (a) PNIPAAm-*g*-UPET, (b) PNIPAAm-*g*-CPET, and (c) PNIPAAm-*g*-HPET, respectively, together with the WCA measurements.

grafted PET textiles and their resistance towards oil adsorption is mainly driven by the increasing entropy of the system *via* the replacement of water molecules at the surface.[62] Due to the hydrophilic character below the LCST, PNIPAAm-*g*-UPET, PNIPAAm-*g*-CPET and PNIPAAm-*g*-HPET revealed anti-oil staining behaviour.

The PNIPAAm hydrogel is intrinsically thermo-responsive.[63–65] Thus, the appearances of the grafted PET textiles were significantly changed above the LCST (Fig. 8iii). When the temperature was increased above the LCST, the PNIPAAm hydrogel switched to a hydrophobic state and became deswollen.[66] Consequently, the hydrophobicity of the surface of the grafted PET promoted more oleophilicity. As a result, the surface of the PNIPAAm hydrogel grafted PET was entirely stained with oil at 45 °C. Clearly, this study has demonstrated that PET textiles grafted with PNIPAAm hydrogels exhibit switchable surface wettability toward oil staining. More importantly, the assessment conducted for up to 5 cycles revealed that the switching from a hydrophilic to hydrophobic state across the LCST was reversible.

Upon a close look at Fig. 8iii, it is found that PNIPAAm-*g*-HPET was completely stained with oil at 45 °C. In contrast, roughly 90% of the PNIPAAm-*g*-UPET surface was covered with oil, while the staining of PNIPAAm-*g*-CPET was only approximately 10%. This reveals that PNIPAAm-*g*-HPET exhibited a relatively higher degree of switchability compared to PNIPAAm-*g*-UPET and PNIPAAm-*g*-CPET. We have noticed that the trend for the degree of switching from hydrophilic/oleophobic to hydrophobic/oleophilic is in agreement with the DG values. This can be explained by the fact that the high DG value of PNIPAAm-*g*-HPET promoted an increased fraction of the hydrogel layer, consequently, the degree of switchability was also easily enhanced.[67]

We also performed WCA measurements at below and above the LCST in order to clarify the wettability and switchability of the as-prepared hydrogel grafted PET textiles, from hydrophobic to hydrophilic, as depicted in Fig. 8ii and iii. At a temperature of 27 °C, all the grafted PET textiles showed good hydrophilic properties to water. The increased hydrophilicity of the grafted PET textiles was noticeable with the decrease in the WCA values from 68.60° for PNIPAAm-*g*-CPET to 48.70° for PNIPAAm-*g*-HPET. In contrast, when raising the temperature up to 45 °C, the WCA of all the grafted PET textiles rapidly increases, and they changed to a hydrophobic state ($\approx 114°$).[53,68] Therefore, the switching of the wettability of the grafted PET textiles is accomplished based on temperature-responsive behaviour. This result was also in good agreement with the DG and anti-staining analysis. From the correlation with the DG, the degree of switchability from oleophobic to oleophilic therefore diminishes according to the following trend: PNIPAAm-*g*-CPET < PNIPAAm-*g*-UPET < PNIPAAm-*g*-HPET.

The resistance of the hydrogel grafted PET textiles towards oil fouling was further investigated based on the time taken for oil to disappear from the surfaces. This test was carried out for 5 cycles at 27 °C, and the results are shown in Fig. 9. Amongst these three grafting samples, the PNIPAAm-*g*-HPET textile showed oil de-staining, with the time taken for the oil to disappear being only around 32–34 seconds. Importantly, the time taken for the oil to disappear from the PNIPAAm-*g*-HPET textile was highly consistent even after testing for 5 cycles. The anti-oil staining behaviour of the PNIPAAm hydrogel grafted PET textiles can be elucidated using the 'water barrier theory'.[69] Below the LCST (27 °C), the PNIPAAm hydrogel is in

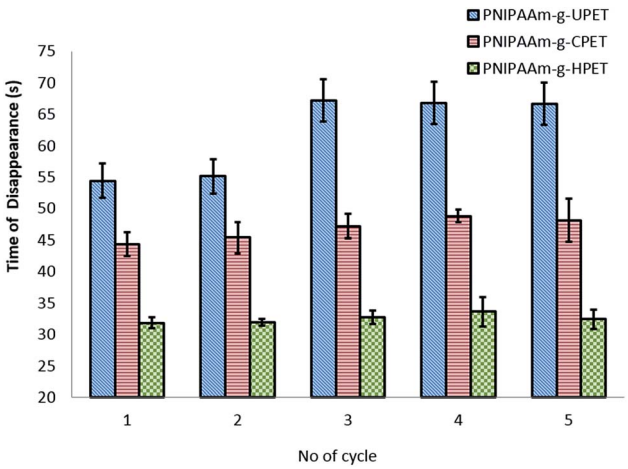

Fig. 9 The anti-oil staining behaviour of untreated and functionalised PNIPAAm-*g*-PET textiles at a temperature of 27 °C based on the time taken for the oil to disappear.

a hydrophilic state and thus it absorbs water and becomes swollen. This theory suggests that the formation of a tightly bound water layer through hydrogen bonding prevented oil from interacting with the hydrogel-grafted PET surfaces. Furthermore, this compact hydration layer created a thermodynamically unfavourable osmotic force and thus repelled the oil from staining the surface.[69]

4. Conclusion

In summary, grafting of PET textiles with PNIPAAm hydrogels was successfully performed *via* photopolymerisation onto the surfaces of HPET > UPET > CPET. The overall results suggest that hydrolysis functionalisation produced more a hydrophilic, rough and reactive surface that yielded the highest DG for PNIPAAm-*g*-HPET. The anti-oil staining tests show that PNIPAAm grafted PET displayed anti-fouling properties. Importantly, the PNIPAAm hydrogel grafted functionalised PET textiles also demonstrated a switchability function from hydrophilicity to hydrophobicity by regulating the temperature in oil staining assessments. To sum up, the impact of different functionalisations of PET textiles on grafting photopolymerisation is very useful for obtaining smart materials with responsive behaviour towards oil staining, which may find further potential application in oil and water separation and smart textiles.

Conflicts of interest

There are no conflicts to declare.

Acknowledgements

This study was supported by the Fundamental Research Grant (FRGS Vote No. 4F960), and funded by the Ministry of Higher Education Malaysia and also the Research University Grant (GUP Vote No. 12H38 and 16H91) funded by the Universiti Teknologi Malaysia.

Notes and references

1 M. M. Bashar, H. Zhu, S. Yamamoto and M. Mitsuishi, *RSC Adv.*, 2017, **7**, 37168–37174.
2 T. Yu, G. Xu, W. Xiwen, J. Yang and J. Hu, *BioResources*, 2014, **9**, 4421–4429.
3 C. Teng, X. Lu, G. Ren, Y. Zhu, M. Wan and L. Jiang, *Adv. Mater. Interfaces*, 2014, **1**, 1400099.
4 Z. Xue, S. Wang, L. Lin, L. Chen, M. Liu, L. Feng and L. Jiang, *Adv. Mater.*, 2011, **23**, 4270–4273.
5 J.-B. Fan, Y. Song, S. Wang, J. Meng, G. Yang, X. Guo, L. Feng and L. Jiang, *Adv. Funct. Mater.*, 2015, **25**, 5368–5375.
6 Q. Wen, J. Di, L. Jiang, J. Yu and R. Xu, *Chem. Sci.*, 2013, **4**, 591–595.
7 P.-C. Chen, L.-S. Wan and Z.-K. Xu, *J. Mater. Chem.*, 2012, **22**, 22727–22733.
8 P. Pi, K. Hou, C. Zhou, X. Wen, S. Xu, J. Cheng and S. Wang, *Mater. Lett.*, 2016, **182**, 68–71.
9 N. G. Eskandar, S. Simovic and C. A. Prestidge, *J. Colloid Interface Sci.*, 2011, **358**, 217–225.
10 M. Li, T. Deng, S. Liu, F. Zhang and G. Zhang, *Appl. Surf. Sci.*, 2014, **297**, 147–152.
11 B. Wang, W. Liang, Z. Guo and W. Liu, *Chem. Soc. Rev.*, 2015, **44**, 336–361.
12 Z. Xue, Y. Cao, N. Liu, L. Feng and L. Jiang, *J. Mater. Chem. A*, 2014, **2**, 2445–2460.
13 Z. Chu, Y. Feng and S. Seeger, *Angew. Chem., Int. Ed.*, 2015, **54**, 2328–2338.
14 J. Wu, W. Wei, S. Zhao, M. Sun and J. Wang, *J. Mater. Sci.*, 2017, **52**, 1194–1202.
15 P.-C. Chen and Z.-K. Xu, *Sci. Rep.*, 2013, **3**, 2776.
16 B. Li, X. Liu, X. Zhang and W. Chai, *Eur. Polym. J.*, 2015, **73**, 374–379.
17 H. Liu, A. Raza, A. Aili, J. Lu, A. AlGhaferi and T. Zhang, *Sci. Rep.*, 2016, **6**, 25414.
18 Y. Zhu, F. Zhang, D. Wang, X. F. Pei, W. Zhang and J. Jin, *J. Mater. Chem. A*, 2013, **1**, 5758–5765.
19 C. Geismann, A. Yaroshchuk and M. Ulbricht, *Langmuir*, 2007, **23**, 76–83.
20 J. Liu, P. Li, L. Chen, Y. Feng, W. He and X. Lv, *Mater. Lett.*, 2016, **185**, 169–172.
21 R. A. Damodar, S.-J. You and H.-H. Chou, *J. Hazard. Mater.*, 2009, **172**, 1321–1328.
22 F. E. Ahmed, L. Boor Singh, N. Hilal and R. Hashaikeh, *Desalination*, 2014, **344**, 48–54.
23 Z.-Y. Luo, K.-X. Chen, D.-C. Mo and S.-S. Lyu, *J. Phys. Chem. C*, 2016, **120**, 11882–11888.
24 R. Gao, Q. Liu, J. Wang, J. Liu, W. Yang, Z. Gao and L. Liu, *Appl. Surf. Sci.*, 2014, **289**, 417–424.
25 X. Du, X. Huang, X. Li, X. Meng, L. Yao, J. He, H. Huang and X. Zhang, *J. Colloid Interface Sci.*, 2015, **458**, 79–86.
26 Z. Weifeng, C. Yingze, L. Na, C. Yuning and F. Lin, *RSC Adv.*, 2014, **4**, 51404–51410.
27 N. Behary, A. Perwuelz, C. Campagne, D. Lecouturier, P. Dhulster and A. S. Mamede, *Colloids Surf., B*, 2012, **90**, 137–143.
28 J. Li, D. Tan, X. Zhang, H. Tan, M. Ding, C. Wan and Q. Fu, *Colloids Surf., B*, 2010, **78**, 343–350.
29 C. Geismann and M. Ulbricht, *Macromol. Chem. Phys.*, 2005, **206**, 268–281.
30 J.-P. Chen, C.-Y. Kuo and W.-L. Lee, *Appl. Surf. Sci.*, 2012, **262**, 95–101.
31 R. Ng, X. Zhang, N. Liu and S.-T. Yang, *Process Biochem.*, 2009, **44**, 992–998.
32 X. Yang, G. Li, T. Cheng, Q. Zhao, C. Ma, T. Tao Xie, T. Li and W. Yang, *J. Appl. Mech.*, 2016, **83**, 1–7.
33 Y. Zhao, S. Zhou, M. Li, A. Xue, Y. Zhang, J. Wang and W. Xing, *Water Res.*, 2013, **47**, 2375–2386.
34 H. Ju, B. D. McCloskey, A. C. Sagle, V. A. Kusuma and B. D. Freeman, *J. Membr. Sci.*, 2009, **330**, 180–188.
35 J. D. Wu, C. Zhang, D. J. Jiang, S. F. Zhao, Y. L. Jiang, G. Q. Cai and J. P. Wang, *RSC Adv.*, 2016, **6**, 24076–24082.
36 S. Mondal and S. R. Wickramasinghe, *Sep. Purif. Technol.*, 2012, **90**, 231–238.
37 B. Liu and J. Hu, *Fibres Text. East. Eur.*, 2005, **13**, 45–49.

38 J. Marchand-Brynaert, M. Deldime, I. Dupont, J.-L. Dewez and Y.-J. Schneider, *J. Colloid Interface Sci.*, 1995, **173**, 236–244.
39 D.-Q. Chen, Y.-Z. Wang, X.-P. Hu, D.-Y. Wang, M.-H. Qu and B. Yang, *Polym. Degrad. Stab.*, 2005, **88**, 349–356.
40 B. Al Meslmani, G. Mahmoud, B. Strehlow, E. Mohr, T. Leichtweiß and U. Bakowsky, *Mater. Sci. Eng., C*, 2014, **43**, 538–546.
41 I. M. Ward, *Trans. Faraday Soc.*, 1957, **53**, 1406–1412.
42 K. Kato, E. Uchida, E.-T. Kang, Y. Uyama and Y. Ikada, *Prog. Polym. Sci.*, 2003, **28**, 209–259.
43 H. Ma, R. H. Davis and C. N. Bowman, *Macromolecules*, 2000, **33**, 331–335.
44 M. Ulbricht, H. Matuschewski, A. Oechel and H.-G. Hicke, *J. Membr. Sci.*, 1996, **115**, 31–47.
45 J. C. Ruiz, C. Alvarez-Lorenzo, P. Taboada, G. Burillo, E. Bucio, K. De Prijck, H. J. Nelis, T. Coenye and A. Concheiro, *Eur. J. Pharm. Biopharm.*, 2008, **70**, 467–477.
46 Y. Wang, C. Lai, H. Hu, Y. Liu, B. Fei and J. H. Xin, *RSC Adv.*, 2015, **5**, 51078–51085.
47 P. Golshaei and O. Güven, *React. Funct. Polym.*, 2017, **118**, 26–34.
48 B. Dong, H. Jiang, S. Manolache, A. C. L. Wong and F. S. Denes, *Langmuir*, 2007, **23**, 7306–7313.
49 M. J. Perez-Roldan, D. Debarnot and F. Poncin-Epaillard, *RSC Adv.*, 2014, **4**, 31409–31415.
50 Y. Shin and D. I. Yoo, *J. Appl. Polym. Sci.*, 2008, **108**, 785–790.
51 J. Škvarla, T. Luxbacher, M. Nagy and M. Sisol, *ACS Appl. Mater. Interfaces*, 2010, **2**, 2116–2127.
52 R. Ou, J. Wei, L. Jiang, G. P. Simon and H. Wang, *Environ. Sci. Technol.*, 2016, **50**, 906–914.
53 B. Xue, L. Gao, Y. Hou, Z. Liu and L. Jiang, *Adv. Mater.*, 2013, **25**, 273–277.
54 P. S. Curti, M. R. d. Moura, W. Veiga, E. Radovanovic, A. F. Rubira and E. C. Muniz, *Appl. Surf. Sci.*, 2005, **245**, 223–233.
55 H. Guo, Y. Ma, P. Sun, S. Cui, Z. Qin and Y. Liang, *RSC Adv.*, 2015, **5**, 63429–63438.
56 S. Roux and S. Demoustier-Champagne, *J. Polym. Sci., Part A: Polym. Chem.*, 2003, **41**, 1347–1359.
57 A. Rahimpour, *Desalination*, 2011, **265**, 93–101.
58 J. Dave, R. Kumar and H. C. Srivastava, *J. Appl. Polym. Sci.*, 1987, **33**, 455–477.
59 V. Muthuvijayan, J. Gu and R. S. Lewis, *Acta Biomater.*, 2009, **5**, 3382–3393.
60 P. D. Peeva, T. Pieper and M. Ulbricht, *J. Membr. Sci.*, 2010, **362**, 560–568.
61 H. Chen, C. Zhao, M. Zhang, Q. Chen, J. Ma and J. Zheng, *Langmuir*, 2016, **32**, 3315–3330.
62 H. Susanto and M. Ulbricht, *Langmuir*, 2007, **23**, 7818–7830.
63 N. Adrus and M. Ulbricht, *React. Funct. Polym.*, 2013, **73**, 141–148.
64 N. Adrus and M. Ulbricht, *Polymer*, 2012, **53**, 4359–4366.
65 N. F. Ayub, S. Hashim, J. Jamaluddin and N. Adrus, *New J. Chem.*, 2017, **41**, 5613–5619.
66 S. Zhou, A. Xue, Y. Zhang, M. Li, J. Wang, Y. Zhao and W. Xing, *J. Membr. Sci.*, 2014, **450**, 351–361.
67 Y. Li, L.-Y. Chu, J.-H. Zhu, H.-D. Wang, S.-L. Xia and W.-M. Chen, *Ind. Eng. Chem. Res.*, 2004, **43**, 2643–2649.
68 Q. Zhong, Y. Y. Chen, S. L. Guan, Q. S. Fang, T. Chen, P. Muller-Buschbaum and J. P. Wang, *RSC Adv.*, 2015, **5**, 38382–38390.
69 C. Zhao, J. Zhao, X. Li, J. Wu, S. Chen, Q. Chen, Q. Wang, X. Gong, L. Li and J. Zheng, *Biomaterials*, 2013, **34**, 4714–4724.